

# Quantification of Histochemical Staining by Color Deconvolution

Arnout C. Ruifrok, Ph.D., and Dennis A. Johnston, Ph.D.

**OBJECTIVE:** To develop a flexible method of separation and quantification of immunohistochemical staining by means of color image analysis.

**STUDY DESIGN:** An algorithm was developed to deconvolve the color information acquired with red-green-blue (RGB) cameras and to calculate the contribution of each of the applied stains based on stain-specific RGB absorption. The algorithm was tested using different combinations of diaminobenzidine, hematoxylin and eosin at different staining levels.

**RESULTS:** Quantification of the different stains was not significantly influenced by the combination of multiple stains in a single sample. The color deconvolution algorithm resulted in comparable quantification independent of the stain combinations as long as the histochemical procedures did not influence the amount of stain in the sample due to bleaching because of stain solubility and saturation of staining was prevented.

**CONCLUSION:** This image analysis algorithm provides a robust and flexible method for objective immunohistochemical analysis of samples stained with up to three different stains using a laboratory microscope, standard RGB camera setup and the public domain program NIH Image. (Analyst Quant Cytol Histol 2001; 23:291-299)

**Keywords:** image processing, computer-assisted; immunohistochemistry; color separation; color deconvolution.

Differential staining of cytoplasm, cell nuclei and other cell organelles, and specific proteins lies at the basis of pathology. One of the most common examples is hematoxylin-eosin staining, with hematoxylin (blue) staining mainly the cell nuclei and eosin (magenta-red) acting as a cytoplasmic stain. In addition to this, the ratio of hematoxylin and eosin staining of the cytoplasm indicates basophilia or acidophilia of the cytoplasm. Another common example of differential staining is the use of immunohistochemistry with, e.g., horseradish-peroxidase staining developed with 3,3' diaminobenzidine (DAB) (brown). Immunohistochemistry techniques can result in highly specific staining of numerous antigens. Slides stained with multiple stains can be used for the cooccurrence and colocalization of different markers—for example, using a proliferation marker like Ki-67 together with a tumor-specific marker like the membrane-localized receptor Her2/Neu, diagnostic of specific breast tumors.

From the Departments of Pathology and Biomathematics, University of Texas M. D. Anderson Cancer Center, Houston, Texas, U.S.A.

Dr. Ruifrok is Assistant Professor, Department of Pathology.

Dr. Johnston is Professor, Department of Biomathematics.

Address reprint requests to: Arnout C. Ruifrok, Ph.D., Department of Pathology, Box 53, M. D. Anderson Cancer Center, 1515 Holcombe Boulevard, Houston, Texas 77030.

**Financial Disclosure:** The authors have no connection to any companies or products mentioned in this article.

Received for publication October 13, 2000.

Accepted for publication February 13, 2001.

The goal of differential staining is to provide indicators of the distribution of the substance or structures to which the stain specifically attaches. The amount of stain attached or deposited will then determine the optical density at stain-specific wavelengths according to the Lambert-Beer law,<sup>1</sup> with optical density proportional to the stain concentration. Although the dyes used for staining the different structures or proteins are visualized as having different colors, they actually mostly have complex overlapping absorption spectra. To simultaneously examine the photometric and morphometric features of one or more structures, the relative contributions of each of the dyes to the resulting absorption spectrum, or the perceived colors, have to be separated. In regions with colocalization of the stains (e.g., staining with hematoxylin and DAB in Ki-67-positive nuclei), the quantification of each stain component cannot be determined at any single wavelength because the optical density at any such wavelength is determined by the total absorption of the multiple stains.

To overcome the problem of separation of the contributions of multiple stains, three approaches have been used:

1. Use of individual components (stains) with nonoverlapping absorption bands. Although some successes have been reported using this approach,<sup>2,3</sup> unfortunately, current cytochemistry and histochemistry still offer only a very limited number of such dyes.

2. Use of narrow-band filters to selectively measure absorption at a dye-specific wavelength. Although a significant improvement in color separation has been made using this technique, it still suffers from partial overlap in the absorption spectra of different dyes.<sup>4-7</sup> Matched filters are needed for every stain used; that may require considerable expense. Even with specifically matched filters, it is difficult to design a system so that each stain appears completely separated into a single color channel. Narrow-band filtering changes the color representation and reduces the color saturation in displays.

3. Use of color transformation techniques based on red-green-blue (RGB) broad-band information from analog or digital three-channel cameras. Considerable success has been shown using color transformation techniques, using either the hue-saturation-intensity (HSI) transformation<sup>6,7</sup> or similar transformations, such as hue-value-chroma<sup>8</sup> or stain-specific transformation.<sup>9,10</sup> A disadvantage of

color transformation techniques is that although the existing color transformations do result in segmentation based on color, they do not result in the separation of the contributions of two or more stains to the resulting color. Areas that are stained with two or more dyes are designated one of the colors, depending on the relative contributions of the stains and threshold settings. This can result in considerable information loss when the above transformation techniques are used.

In histologic and cytologic staining it is hardly ever the case that areas are stained for one color only. This means that considerable information is lost when the above transformation techniques are used. Therefore, we developed a novel color-deconvolution method that makes use of the broad-band RGB information of standard analog or digital three-channel cameras. The method can be used for separation of practically every combination of two or three colors, provided that the colors are sufficiently different in their red, green or blue absorption characteristics. As the RGB sensitivity of cameras is matched to the RGB sensitivity of the human visual system, virtually every set of three colors that can be seen as different colors by eye also can be separated by the color-deconvolution method. The method is based on orthonormal transformation of the original RGB image, depending on user-determined color information about the three colors. The method provides the possibility to determine staining densities, even in areas where multiple stains are colocalized, making it possible not only to determine surface area and overall absorption in areas with a specific color but also to determine densities and ratios of densities of stains in each area. After color deconvolution, images can be reconstructed for each stain separately and be used for densitometry and texture analysis for each stain, using standard imaging methods.

## Theory

### Color Representation

In this discussion we assume a video microscopy system with an RGB camera, assuming that gray levels in each of the RGB channels are linear with brightness or transmission  $T$ , with  $T$  being  $I/I_0$ , with  $I_0$  being the incident light and  $I$  the transmitted light. This assumption is reasonably accurate for CCD cameras with a gamma of 1.0.

Each pure stain will be characterized by a specific absorption factor,  $c$ , for the light in each of the three RGB channels. The detected intensities of light

transmitted through a specimen and the amount (A) of stain with the absorption factor,  $c$ , are described by Lambert-Beer's law,<sup>1</sup>

$$I_c = I_{0,c} \exp(-Ac_c),$$

with  $I_{0,c}$  the intensity of light entering the specimen,  $I_c$  the intensity of light detected after passing the specimen and subscript  $c$  indicating the detection channel. This means that the transmission of light, and therefore the gray values of each channel, depend on concentration of stain in a nonlinear way.

In the RGB model, the intensities  $I_R$ ,  $I_G$  and  $I_B$  are obtained by the camera for each pixel. Because the relative intensity in each of the channels depends on the concentration of stain in a nonlinear way,<sup>11</sup> the intensity values of the image cannot directly be used for separation and measurement of each of the stains. However, the optical density (OD) for each channel can be defined as

$$OD_c = -\log_{10}(I_c/I_{0,c}) = A \cdot c_c.$$

The OD for each channel is linear with the concentration of absorbing material and can therefore be used for separation of the contributions of multiple stains in a specimen.

Each pure stain will be characterized by a specific OD for the light in each of the three RGB channels, which can be represented by a  $3 \times 1$  OD vector describing the stain in the OD-converted RGB color space. For example, measurements of a sample stained with only hematoxylin resulted in OD values of 0.18, 0.20 and 0.08 for the R, G and B channels, respectively.

The length of the vector will be proportional to the amount of stain, while the relative values of the vector describe the actual OD for the detection channels. In the case of three channels, the color system can be described as a matrix of the form

$$\begin{bmatrix} p_{11} & p_{12} & p_{13} \\ p_{21} & p_{22} & p_{23} \\ p_{31} & p_{32} & p_{33} \end{bmatrix}$$

With every row representing a specific stain and every column representing the OD as detected by the red, green and blue channel for each stain. Stain-specific values for the OD in each of the three channels can be easily determined by measuring relative absorption for red, green and blue on slides stained with a single stain. An example of the OD matrix for the combination of hematoxylin, eosin and DAB is:

R	G	B	
0.18	0.20	0.08	Hematoxylin
0.01	0.13	0.01	Eosin
0.10	0.21	0.29	DAB.

### Color Deconvolution

To perform separation of the stains, we have to do an orthonormal transformation of the RGB information to obtain independent information about each stain's contribution. The transformation has to be orthogonal to achieve independent information about each of the stains; the transformation has to be normalized to achieve correct balancing of the absorption factor for each separate stain.

For normalization, we divide each OD vector by its total length,

$$\hat{p}_{11} = p_{11} / \sqrt{p_{11}^2 + p_{12}^2 + p_{13}^2},$$

$$\hat{p}_{21} = p_{21} / \sqrt{p_{21}^2 + p_{22}^2 + p_{23}^2},$$

$$\hat{p}_{31} = p_{31} / \sqrt{p_{31}^2 + p_{32}^2 + p_{33}^2},$$

and so forth,

resulting in a normalized OD matrix, M:

$$\begin{bmatrix} \hat{p}_{11} & \hat{p}_{12} & \hat{p}_{13} \\ \hat{p}_{21} & \hat{p}_{22} & \hat{p}_{23} \\ \hat{p}_{31} & \hat{p}_{32} & \hat{p}_{33} \end{bmatrix}.$$

The normalized OD matrix, M, for the above combination of hematoxylin, eosin and DAB is:

$$\begin{bmatrix} 0.65 & 0.70 & 0.29 \\ 0.07 & 0.99 & 0.11 \\ 0.27 & 0.57 & 0.78 \end{bmatrix}.$$

If  $C$  is the  $3 \times 1$  vector for amounts of the three stains at a particular pixel, then the vector of OD levels detected at that pixel is  $y = CM$ .

From the above it is clear that  $C = M^{-1}[y]$ . This means that multiplication of the OD image with the inverse of the OD matrix, which we define as the color-deconvolution matrix,  $D$ , results in orthogonal representation of the stains forming the image:

$$C = D[y].$$

$D$ , corresponding to  $M$  for the hematoxylin, eosin and DAB matrix, is:

$$\begin{bmatrix} 1.88 & -0.07 & -0.60 \\ -1.02 & 1.13 & -0.48 \\ -0.55 & -0.13 & 1.57 \end{bmatrix},$$

In this matrix, the diagonal elements are greater than unity, while the off-diagonal elements are neg-

ative. The above equation implies that the corrected OD level values for each stain are formed by subtracting a portion of the green OD and blue OD from the enhanced red OD to obtain the hematoxylin OD, subtracting a portion of the red OD and blue OD from the enhanced green OD to obtain the eosin OD and subtracting a portion of the red OD and green OD from the enhanced blue OD to obtain the DAB OD. In case the stains used would be pure red, green and blue, the above matrix would be the unity matrix.

Results of experiments using the above method are presented below. Combinations of different staining intensities on the same slides were performed to test the influence of different levels of eosin counterstain on the quantification of DAB and hematoxylin.

## Materials and Methods

### Specimens

Sections from a breast tumor specimen were stained for Her2/neu expression with Her2/neu-specific antibody (Oncogene Science, Cambridge, Massachusetts, U.S.A.) and DAB chromogen (Biogenics, Napa, California, U.S.A.). Counterstaining was performed with Mayer's Hematoxylin (Richard Allan, Kalamazoo, Michigan, U.S.A.) for three to five minutes and eosin (Polyscientific, Bay Shore, New York, U.S.A.) for different periods under visual control. Sections from a lung tissue specimen were stained with Mayer's Hematoxylin (Richard Allan) for three to five minutes and eosin (Polyscientific) for different periods under visual control. For determination of the effect of different eosin-staining levels on DAB and hematoxylin staining measurements, slides were destained in 95% alcohol or demineralized water and restained with eosin for different periods to reach a range of eosin staining intensities. Corresponding areas of slides were analyzed after each staining step, and stained area, OD and integrated OD (IOD) were determined.

### Image Acquisition

A Leica DMLB microscope (Leica Microsystems Inc., Deerfield, Illinois, U.S.A.) was equipped with a Hamamatsu C5810 chilled three-chip color CCD camera (Hamamatsu, Bridgewater, New Jersey, U.S.A.) interfaced with an IBM computer (International Business Machines Corporation, Armonk, New York, U.S.A.) equipped with a Matrox Meteor digitizer board (Matrox Electronic Systems Ltd., Dorval, Quebec, Canada).

Light and camera settings were standardized, resulting in average background values of  $20 \pm 5$  (mean  $\pm$  SD, scale 0–255 from white to black) for the red, green and blue channels. Linearity of the image-acquisition setup was tested using a stepped neutral density filter and was found to be linear with light intensity for all three colors within 2% over the whole dynamic range of the camera (correlation coefficients of the OD with grayscale values for red, green and blue:  $R > .996$ ,  $R^2 > .993$ ). The images were captured with  $20\times$  (lung tissue) and  $40\times$  (breast tissue) objective lenses.

### Image Processing

The 24-bit RGB images were transferred to a Macintosh G4 computer (Apple Computer, Cupertino, California, U.S.A.) and processed and analyzed using NIH image version 1.62, developed at the National Institutes of Health and available on the internet from <http://rsb.info.nih.gov/ni-image/>. Custom macros were written for background correction and transformation from intensity to OD to determine the color vectors for the different stains, for calculation of the color-deconvolution matrix and for the actual color deconvolution of the images. The stored image of an empty field was used for determination of the light entering at each pixel ( $I_{0,c}$ ), implicitly correcting for unequal illumination background subtraction.

### Test of the System Performance

To test the performance of the deconvolution algorithm, different staining combinations were quantified on the same areas of tissue sample. Quantification of DAB staining was performed by repeated measurement of samples stained with only DAB, DAB plus hematoxylin and DAB plus hematoxylin plus eosin at different levels. To test the influence of eosin staining on the quantification of hematoxylin, repeated measurements were performed with several levels of eosin staining. The interaction of the stains with respect to quantification of each separated stain was compared using the analysis of covariance. This was accomplished using SPSS (SPSS, Inc., Chicago, Illinois, U.S.A.) and the custom program AOC ([www.odin.mdacc.tmc.edu](http://www.odin.mdacc.tmc.edu)). This procedure follows the general plan described by Zar.<sup>12</sup> Descriptive comparison of performance was done using the measures mean shift, scale factor (ratio of the SDs), precision (equal to the correlation coefficient), accuracy (mixture of the means and SDs) and concordance (product of precision and accuracy), as

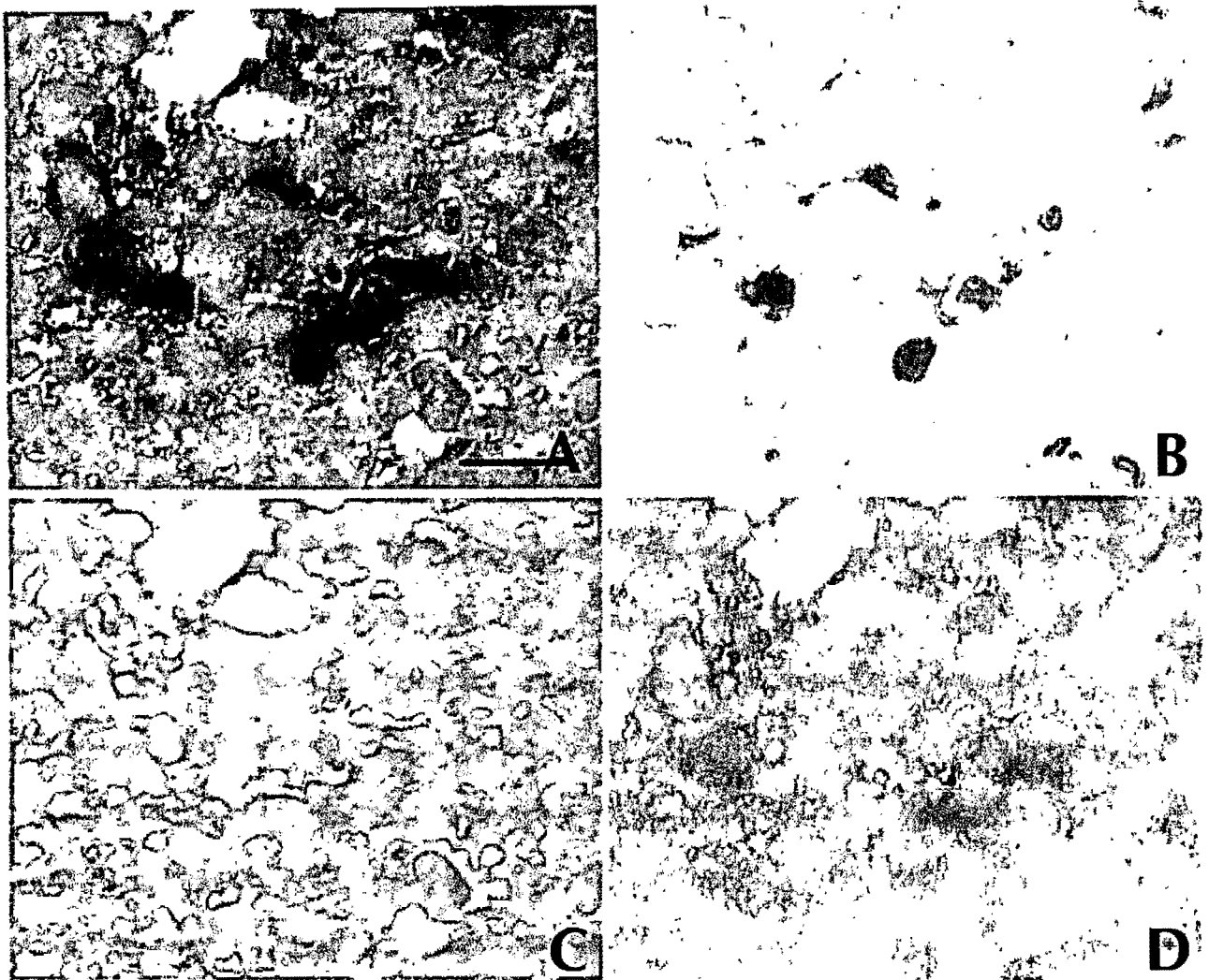


**Figure 1** (A) Photomicrograph of a breast tissue slide stained with DAB (brown), hematoxylin (blue) and eosin (magenta). (B–D) Color-deconvolution results separating the contributions of hematoxylin (B), eosin (C) and DAB (D) to the original image ( $\times 40$ , bar = 20  $\mu\text{m}$ ).

described by Fisher and van Belle.<sup>13</sup> With optimal reproducibility, the mean shift centers around 0, the scale factor centers around 1, and precision, accuracy and concordance maximize to 1.

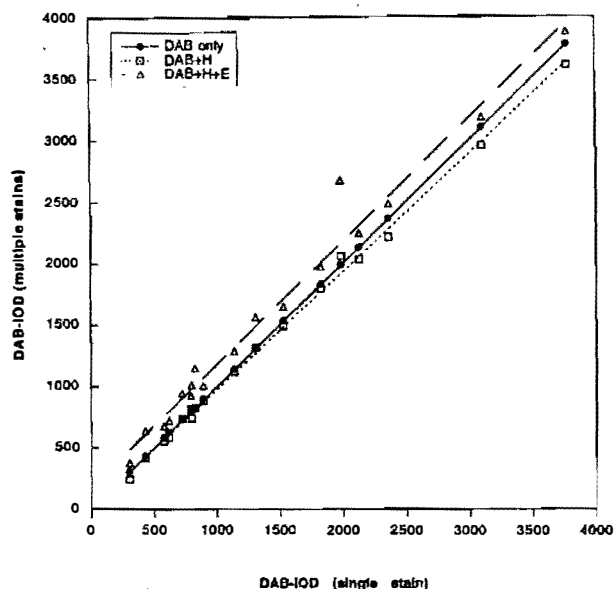
### Results

Figure 1 shows a representative example of DAB, hematoxylin and eosin staining before and after color deconvolution. The result is a set of three images showing continuous representation of the three contributing stains.

To test the performance of the color-deconvolution algorithm under different circum-

stances, we compared quantification of the stains using different combinations and concentrations. Descriptive comparison of performance was done using the measures mean shift, scale factor, precision, accuracy and concordance, as described by Fisher and van Belle.<sup>13</sup> With optimal reproducibility, the mean shift centers around 0, the scale factor centers around 1, and precision, accuracy and concordance maximize to 1.

Addition of hematoxylin staining to the slides did not result in significant changes in the measured IOD of DAB staining (Figure 2). The mean shift of the IOD measurements was  $<0.05$ , and the



**Figure 2** Influence of combinations of hematoxylin (H) and eosin (E) on quantification of DAB in breast tissue sections. The IOD measurements for DAB in areas stained with different chromogen combinations were plotted against the IOD measurements for DAB staining alone in the same areas.

scale factor was  $>0.95$ . With a precision of  $>0.99$ , this resulted in an accuracy of  $>0.99$  and concordance of  $>0.99$ .

When hematoxylin and eosin both were added to the DAB-stained slides, no difference in slope was observed ( $P = .281$ ), but a significant mean shift ( $P < .001$ ) was seen (Figure 2). This indicates a difference in level but no interaction of stains that would change the rate of DAB quantification. Although after addition of eosin a significant mean shift to higher IOD values was observed, the scale factor was 0.95. Because of the high precision (0.99) and the high accuracy (0.98), the resulting concordance (0.97) still was high.

To further study the influence of eosin staining on the DAB quantification, we measured the DAB IOD with different levels of eosin counterstain. Eosin staining was added, or "bleached," by incubating the slides in 95% alcohol or distilled water until an appreciable reduction in eosin staining was observed. This way, eosin concentration was increased and reduced to about 75% and 40% of the initial concentration. There were no significant differences in slope ( $P = .738$ ) or mean ( $P = .193$ ) of DAB quantifications, indicating that the three eosin levels did not significantly interfere with DAB

quantification (Figure 3). Even after these multiple rounds of processing, the DAB measurements showed precision, accuracy and concordance of  $>0.99$ , with mean shifts of  $<0.1$  and scale factors of 0.98–1.00. These data clearly show the stability of the stain and robustness of the quantification procedure.

Finally, to study the interaction between hematoxylin and eosin quantification, we stained and destained sections of lung tissue stained with hematoxylin and different levels of eosin. The results of these experiments are shown in Figure 4. Quantification of hematoxylin decreased after manipulation of eosin staining. The first eosin staining resulted mainly in a mean shift of the measurements to lower values, with a mean shift value of 0.59, while the scale factor was 1.06. With precision of  $>0.99$ , this resulted in accuracy and concordance of 0.84.

To determine whether this was the result of interference of the colors in the quantification process or came from actual reduction of the staining due to technical artifacts (bleaching of hematoxylin during eosin staining), we repeatedly destained and

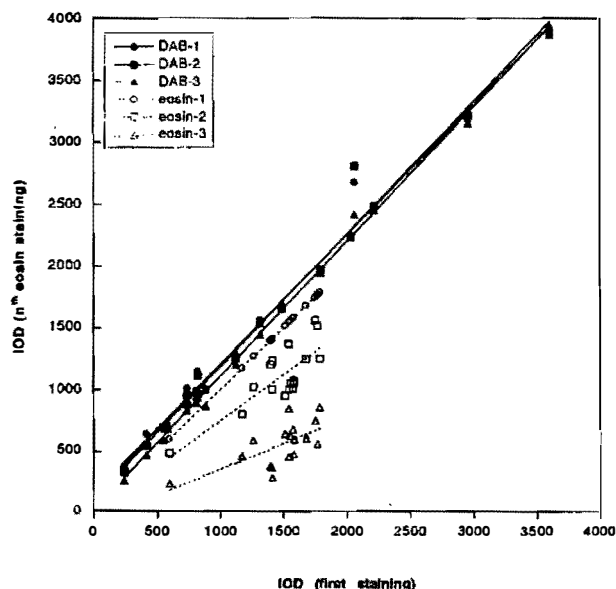


**Figure 3** Influence of different levels of eosin staining on the quantification of DAB and eosin in breast tissue sections. The IOD measurement for DAB and eosin in areas stained with different amounts of eosin was plotted against the IOD measurements for DAB and eosin staining (first staining) alone in the same areas. In the first eosin staining step, eosin was added (100%); in the following two steps increasing amounts of eosin were bleached from the slide (to about 75% and 40%).

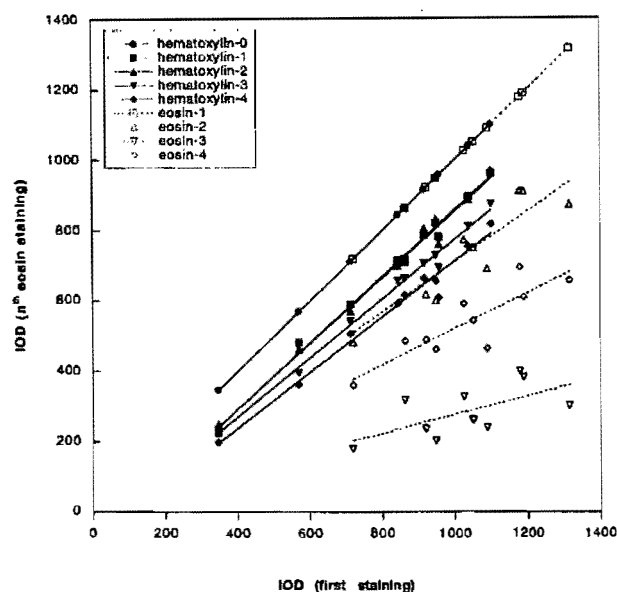


**Figure 4** Influence of different levels of eosin staining on quantification of hematoxylin in lung tissue sections. The IOD measurement for hematoxylin and eosin in areas stained with different amounts of eosin was plotted against the IOD measurements for DAB and eosin staining (first staining) alone in the same areas. In the first eosin staining step eosin was added (100%), in the second and third steps increasing amounts of eosin were bleached from the slide (to about 71% and 27%), and in the fourth step eosin was added again (to about 51%).

restained the samples with eosin. The slopes were significantly different ( $P = .0096$ ), with the change showing a dose/response relationship with the repeated treatments (adding or bleaching) of eosin, reducing the slope (0.943 to 0.792, respectively) versus hematoxylin alone. This happened regardless of whether the eosin staining increased or decreased. Therefore, we conclude that the decrease in hematoxylin measurements was the result of reduction of the amount of stain during processing, due to bleaching in aqueous media, not due to interference of quantification of the two stains.

### Discussion

Image analysis for the quantification of differential cytochemical or immunohistochemical staining has the advantage over biochemical assays and flow cytometry that it is nondestructive and that information concerning the relation between morphology and the cell organelle or protein under study is maintained. In addition, automated analysis is faster, more objective and less laborious than visual

examination. Segmentation and density measurements can be performed using interactive as well as computer-determined thresholds. However, overlap in spectral absorption by the stains used can be a major problem.

Several methods have been proposed in attempts to obtain independent information about the stain concentrations in histologic and cytologic specimens. Some of the systems try to limit either the spectral overlap of the stains (monochromatic dyes) or the spectral overlap of the detection system (narrow band filters). The use of monochromatic dyes was limited by the availability of such dyes. The use of a narrow-band filter sometimes requires expensive filters and results in a reduced signal, which may compromise the signal-to-noise ratio of the image and thereby reduce the reliability of the measurements. Even with the use of narrow-band filters, overlap in absorption in the specific wavelength regions may occur, resulting in incomplete elimination of the respective chromogens.<sup>7</sup>

Another category of methods uses basic RGB information or a transformation of this information into, e.g., HSI or color-specific components for segmentation of the image in areas of different colors. These color separation techniques use one of the transformed values (e.g., hue or chroma) for color classification by some thresholding technique. The classification of pixels is exclusive; each pixel is designated as one of the targeted colors or hues. However, as absorption of different colors contributes to the overall red, green and blue absorption and as such also to the overall hue, saturation and intensity, color separation can no longer be achieved reliably.

We present a color deconvolution algorithm that uses the information on all contributing colors. It can be used on standard RGB images, as acquired with a standard, three-channel analog or digital camera. Processing can be performed quickly and easily on a Macintosh computer using custom macros written for the public domain program NIH image. This means that for the price of a good three-chip CCD camera and digitizer board, it is possible to perform quantitative histochemical analysis.

The present method of color deconvolution allows the separate presentation of stain components even if the stains show overlapping spectral absorption spectra as well as colocalization. Measurement of the color vectors of the specific stains can easily be determined on single-stained specimens. In case of interaction between stains, the user can-

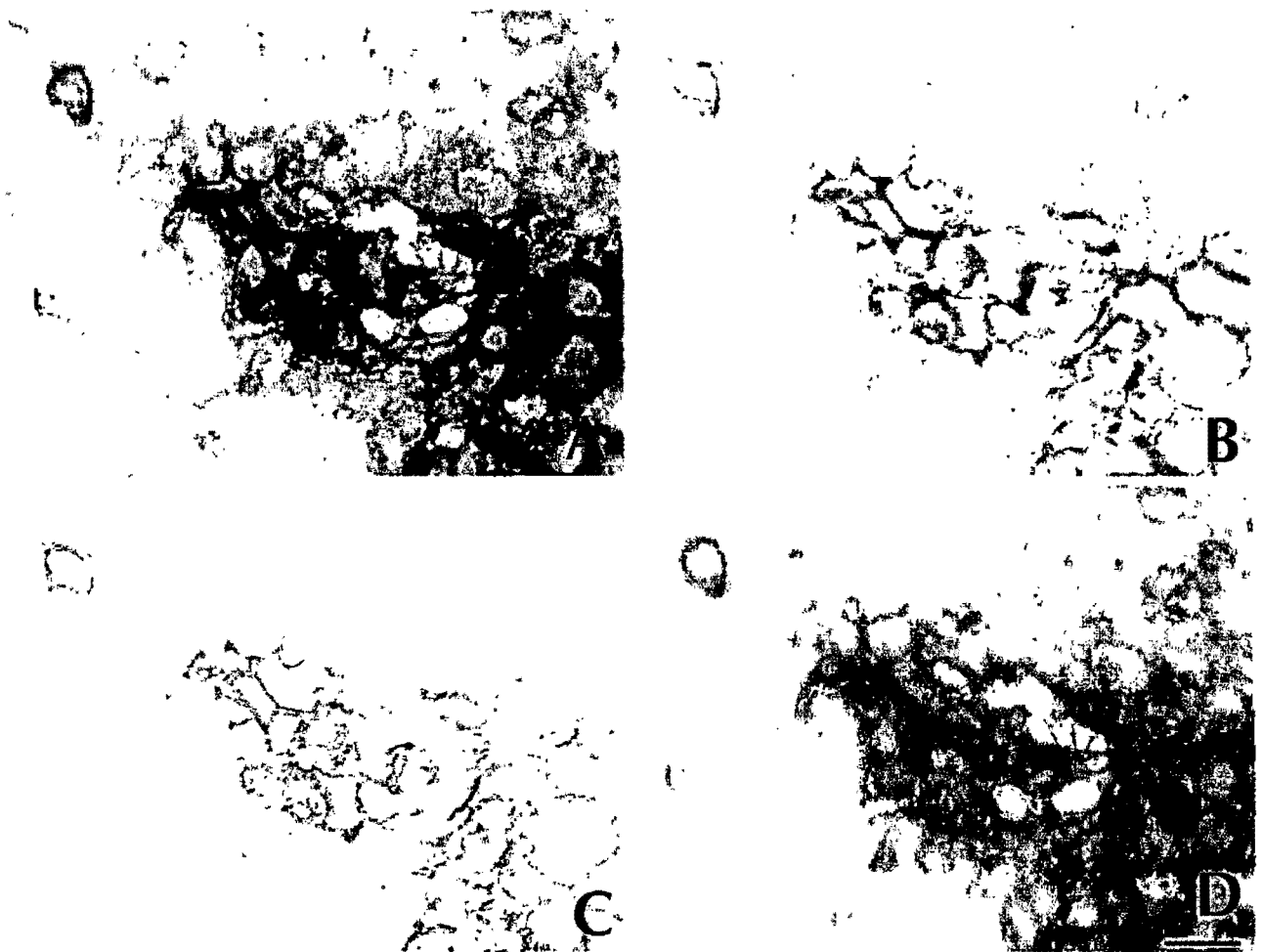


**Figure 5** (A) Photomicrograph of a breast tissue slide stained with saturating levels of DAB (brown). (B–D) Color-deconvolution results showing the apparent contribution of hematoxylin (B) and eosin (C) ( $\times 40$ , bar = 20  $\mu\text{m}$ ).

select areas of the multiple-stained slides as representative of the color to be measured. The method overcomes the disadvantages of filtering techniques or RGB or HSI color segmentation techniques. The color deconvolution technique allows insight into the biochemical composition of a tissue because it leads to accurate quantification of the relative distribution of each stain.

As shown above, addition of hematoxylin or eosin to DAB staining hardly influences DAB quantification. Eosin staining also does not seem to influence hematoxylin quantification, apart from the histotechnical complication of bleaching the stain.

Because hematoxylin and eosin are soluble in aqueous media, it was not possible to reliably determine the influence of the addition of DAB to

eosin or hematoxylin quantification. However, we did apply the above algorithm to DAB-only-stained sections to make an estimate of the possible (erroneous) contribution of DAB staining to hematoxylin and eosin quantification. Erroneous deconvolution may especially be the result of saturation of staining and signal detection. As it is clear that saturation of a signal makes it impossible to perform accurate quantification, all color separation techniques, including the present one, will result in erroneous measurements when saturation takes place. Therefore, extremely dark DAB staining may result in an erroneous measurement of a "hematoxylin" signal and "eosin" signal even if these colors are not actually present. We had extremely dark DAB staining in some areas of the



slides; an example is given in Figure 5. As can be clearly seen, the very dark areas of the DAB-stained slide also contributed to the hematoxylin and eosin image. As a result of this, the possible contribution of DAB-saturated areas to the measured IOD for hematoxylin reached an average of 65%. Eosin quantification was less influenced by this phenomenon: only about 8% of the IOD measured at the lowest eosin staining level could possibly have contributed to saturation of DAB staining, while the mean amount was only 3% for the darkest eosin staining.

The present data show that chromogen quantification is not significantly influenced by addition of a second or third color but mainly by the stability of the chromogens used in the staining procedure as long as saturation of staining in each of the colors is prevented. This means that using the presented color separation technique, the reliability of the measurements depends mainly on the quality of the sample input, stressing the importance of the use of standard methods, inclusion of standard samples and prevention of signal saturation.

### Acknowledgments

The authors thank Sejal Patel and Abha Khana for their expert technical assistance.

### References

1. Jähne B: Practical Handbook on Image Processing for Scientific Applications. Boca Raton, Florida, CRC Press, 1997, pp 76–82
2. Bacus S, Flowers JL, Press MF, Bacus JW, McCarty KS: The evaluation of estrogen receptor in primary breast carcinoma by computer-assisted image analysis. *Am J Clin Pathol* 1988; 90:233–239
3. Bacus SS, Goldschmidt R, Chin D, Weinberg D, Bacus JW: Biological grading of breast cancer using antibodies to proliferating cells and other markers. *Am J Pathol* 1989;135: 783–792
4. Zhou R, Parker DL, Hammond EH: Quantitative peroxidase-antiperoxidase complex-substrate mass determination in tissue sections by a dual wavelength method. *Analyt Quant Cytol Histol* 1992;14:73–80
5. Zhou R, Hammond EH, Parker DL: A multiple wavelength algorithm in color image analysis and its application in stain decomposition in microscopy images. *Med Phys* 1996;23: 1977–1986
6. Lehr H-A, Mankoff DA, Corwin D, Santeusano G, Gown AM: Application of Photoshop-based image analysis to quantification of hormone receptor expression in breast cancer. *J Histochem Cytochem* 1997;11:1559–1565
7. Lehr H-A, van der Loos CM, Teeling P, Gown AM: Complete chromogen separation and analysis in double immunohistochemical stains using Photoshop-based image analysis. *J Histochem Cytochem* 1999;47:119–125
8. Kai M, Nunobiki O, Taniguchi E, Sakamoto Y, Kakudo K: Quantitative and qualitative analysis of stain color using RGB computer color specification. *Analyt Quant Cytol Histol* 1999;21:477–480
9. Ruifrok AC: Quantification of immunohistochemical staining by color translation and automated thresholding. *Analyt Quant Cytol Histol* 1997;19:107–113
10. Montorini R, Diamanti L, Thompson D, Bartels HG, Bartels PH: Analysis of the capillary architecture in the precursors of prostate cancer: Recent findings and new concepts. *Eur Urol* 1996;30:191–200
11. Van der Laak JAWM, Pahiplatz MMM, Hanselaar AGJM, de Wilde PCM: Hue-saturation-density (HSD) model for stain recognition in digital images from transmitted light microscopy. *Cytometry* 2000;39:275–284
12. Zar JH: Biostatistical Analysis. Fourth edition. Upper Saddle River, New Jersey, Prentice-Hall, 1999, pp 369–375
13. Fisher LD, van Belle G: Biostatistics: A Methodology for the Health Sciences. New York, John Wiley & Sons, 1993, pp 897–901